



**Metallurgical Examination of a Failed AH-64D Pilot  
Cyclic Stick (Part Number 7-511512001-3)**

**by Victor Champagne and Scott Grendahl**

**ARL-TR-3272**

**August 2004**

## **NOTICES**

### **Disclaimers**

The findings in this report are not to be construed as an official Department of the Army position unless so designated by other authorized documents.

Citation of manufacturer's or trade names does not constitute an official endorsement or approval of the use thereof.

Destroy this report when it is no longer needed. Do not return it to the originator.

# **Army Research Laboratory**

Aberdeen Proving Ground, MD 21005-5069

---

---

**ARL-TR-3272**

**August 2004**

---

## **Metallurgical Examination of a Failed AH-64D Pilot Cyclic Stick (Part Number 7-511512001-3)**

**Victor Champagne and Scott Grendahl  
Weapons and Materials Research Directorate, ARL**

## Report Documentation Page

*Form Approved*  
OMB No. 0704-0188

Public reporting burden for this collection of information is estimated to average 1 hour per response, including the time for reviewing instructions, searching existing data sources, gathering and maintaining the data needed, and completing and reviewing the collection information. Send comments regarding this burden estimate or any other aspect of this collection of information, including suggestions for reducing the burden, to Department of Defense, Washington Headquarters Services, Directorate for Information Operations and Reports (0704-0188), 1215 Jefferson Davis Highway, Suite 1204, Arlington, VA 22202-4302. Respondents should be aware that notwithstanding any other provision of law, no person shall be subject to any penalty for failing to comply with a collection of information if it does not display a currently valid OMB control number.  
**PLEASE DO NOT RETURN YOUR FORM TO THE ABOVE ADDRESS.**

<b>1. REPORT DATE (DD-MM-YYYY)</b> August 2004		<b>2. REPORT TYPE</b> Final		<b>3. DATES COVERED (From - To)</b> January 2003–February 2003	
<b>4. TITLE AND SUBTITLE</b> Metallurgical Examination of a Failed AH-64D Pilot Cyclic Stick (Part Number 7-511512001-3)				<b>5a. CONTRACT NUMBER</b>	
				<b>5b. GRANT NUMBER</b>	
				<b>5c. PROGRAM ELEMENT NUMBER</b>	
<b>6. AUTHOR(S)</b> Victor Champagne and Scott Grendahl				<b>5d. PROJECT NUMBER</b> W31P4Q3R71203	
				<b>5e. TASK NUMBER</b>	
				<b>5f. WORK UNIT NUMBER</b>	
<b>7. PERFORMING ORGANIZATION NAME(S) AND ADDRESS(ES)</b> U.S. Army Research Laboratory ATTN: AMSRD-ARL-WM-MC Aberdeen Proving Ground, MD 21005-5069				<b>8. PERFORMING ORGANIZATION REPORT NUMBER</b> ARL-TR-3272	
<b>9. SPONSORING/MONITORING AGENCY NAME(S) AND ADDRESS(ES)</b> U.S. Army Aviation and Missile Command Redstone Arsenal Huntsville, AL 35898				<b>10. SPONSOR/MONITOR'S ACRONYM(S)</b>	
				<b>11. SPONSOR/MONITOR'S REPORT NUMBER(S)</b>	
<b>12. DISTRIBUTION/AVAILABILITY STATEMENT</b> Approved for public release; distribution is unlimited.					
<b>13. SUPPLEMENTARY NOTES</b>					
<b>14. ABSTRACT</b> The U.S. Army Research Laboratory was requested by the U.S. Aviation and Missile Command (AMCOM) to examine a pilot cyclic stick (part number [P/N] 7-511512001-3) and a copilot cyclic stick (P/N 7-511515001-3) taken from an AH-64D Apache helicopter, which crashed at Ft. Rucker, AL. The pilot stick was received broken into two pieces while the copilot stick was cracked, but not completely separated. While this investigation focused on the pilot stick, findings from the copilot stick were included at times for comparative purposes. The objective of this failure analysis was to determine if any metallurgical evidence existed that suggested that the fractured pilot stick might have contributed to the cause of the crash or whether it occurred as a result of the mishap. The metallurgical findings suggested that the pilot stick fractured during a single event. There was no evidence of fatigue observed on the fracture surface of the pilot stick. The fracture morphology consisted primarily of ductile dimples, indicative of overload conditions. There existed some areas that were indicative of cleavage fracture, but nothing that would suggest a fatigue-induced failure.					
<b>15. SUBJECT TERMS</b> failure analysis, 6061-T6 A1, welding					
<b>16. SECURITY CLASSIFICATION OF:</b>			<b>17. LIMITATION OF ABSTRACT</b>  UL	<b>18. NUMBER OF PAGES</b>  34	<b>19a. NAME OF RESPONSIBLE PERSON</b> Victor Champagne
<b>a. REPORT</b> UNCLASSIFIED	<b>b. ABSTRACT</b> UNCLASSIFIED	<b>c. THIS PAGE</b> UNCLASSIFIED			<b>19b. TELEPHONE NUMBER (Include area code)</b> 410-306-0822

Standard Form 298 (Rev. 8/98)  
Prescribed by ANSI Std. Z39.18

---

## Contents

---

<b>List of Figures</b>	<b>iv</b>
<b>List of Tables</b>	<b>v</b>
<b>1. Introduction</b>	<b>1</b>
<b>2. Objective</b>	<b>1</b>
<b>3. Visual Examination</b>	<b>1</b>
<b>4. Metallographic Examination</b>	<b>11</b>
4.1 Eddy Current Electrical Conductivity .....	13
4.2 Hardness Testing .....	13
4.3 Chemistry .....	13
<b>5. Scanning Electron Microscopy (SEM)</b>	<b>17</b>
<b>6. Conclusion</b>	<b>22</b>
<b>7. Recommendations</b>	<b>22</b>
<b>Distribution List</b>	<b>25</b>

---

## List of Figures

---

Figure 1. The fractured AH-64D pilot cyclic stick as received by ARL. ....	2
Figure 2. Enlargement of the fracture area on the pilot stick.....	2
Figure 3. Detail of the pilot stick fractured area. ....	3
Figure 4. The fractured AH-64D copilot cyclic stick as received by ARL. ....	4
Figure 5. Detail of the copilot stick crack at the elbow to tube weld. ....	4
Figure 6. The fracture halves of the pilot cyclic stick.....	5
Figure 7. Lack of penetration observed on the tube side fracture half. ....	5
Figure 8. Lack of penetration on the tube side at location G on the drawing.....	6
Figure 9. Lack of penetration on the tube side at location F on the drawing.....	6
Figure 10. Montage of the fracture surface of the pilot cyclic stick. ....	7
Figure 11. Montage from figure 10 depicting the area that should be welded. ....	8
Figure 12. Montage from figure 10 depicting the area that was not welded. ....	8
Figure 13. Elbow side fracture half depicting failure origins. ....	9
Figure 14. Elbow side fracture half depicting large gas void failure origin, from left side of figure 13.....	9
Figure 15. Elbow side fracture half depicting failure origin from cracks and a gas void at the root of the weld, from middle of figure 13. ....	10
Figure 16. Elbow side fracture half depicting failure origin from large cracks at weld root, from right of figure 13. ....	10
Figure 17. Elbow side cross section through the weld; the white line depicts what would be a 100% penetration weld. ....	11
Figure 18. Tube side cross section through the weld.....	12
Figure 19. Tube side cross section of base material. ....	12
Figure 20. EDS spectrum for the 4043 welding filler rod. ....	15
Figure 21. EDS spectrum for the 4643 welding filler rod. ....	16
Figure 22. EDS spectrum for the filler metal on the welded pilot stick. ....	16
Figure 23. SEM fractograph showing the morphology predominant on the cyclic stick. ....	18
Figure 24. SEM fractograph showing dimpled morphology with directionality.....	18
Figure 25. SEM fractograph showing quasi-cleavage morphology.....	19
Figure 26. SEM fractograph showing fracture origin from figure 14.....	19
Figure 27. SEM fractograph showing fracture origin from figure 15.....	20
Figure 28. SEM fractograph showing fracture origin from figure 16.....	20

Figure 29. SEM fractograph showing unfused material from figure 26.....	21
Figure 30. SEM fractograph showing enlargement of figure 27. ....	21
Figure 31. SEM fractograph showing enlargement of figure 28. ....	22
Figure 32. SEM fractograph showing typical gas voids on the surface.....	23
Figure 33. SEM fractograph showing additional typical gas voids on the surface.....	23

---

## List of Tables

---

Table 1. Electrical conductivity for 6061-T6 and the pilot stick tube material. ....	13
Table 2. Hardness for 6061-T6 and the pilot stick tube/elbow material.....	14
Table 3. Hardness for 6061-T6 and the pilot stick weldment profiles.....	14
Table 4. Chemical composition of pilot stick tube and elbow material in weight-percent. ....	14
Table 5. Chemical composition of the weld bead and specified weld rods (EDS analysis).....	17
Table 6. Chemical composition of the weld bead and specified weld rods (DCP analysis).....	17

INTENTIONALLY LEFT BLANK.



---

## **1. Introduction**

---

The U.S. Army Research Laboratory (ARL) was requested by the U.S. Aviation and Missile Command (AMCOM) to examine a pilot cyclic stick (part number [P/N] 7-511512001-3) and a copilot cyclic stick (P/N 7-511515001-3) taken from an AH-64D Apache helicopter, which crashed at Ft. Rucker, AL. The pilot stick was received broken in two pieces, while the copilot stick was cracked, but not completely separated. While this investigation focused on the pilot stick, findings from the copilot stick are included at times for comparative purposes.

The failure analysis of the Apache cyclic stick commenced at ARL on 21 January 2003. In attendance were Michael Schachte representing Boeing-Mesa and George Liu representing AMCOM-Huntsville. Scott Grendahl and Victor Champagne of ARL conducted the analysis. Ronny Fritz from the Corpus Christ Army Depot Aircraft Accident Board was not present but was contacted by Victor Champagne prior to the investigation to obtain approval to proceed. Approval was granted.

Visual and optical examinations of the parts were conducted on the pilot and copilot stick on 21 January 2003. Scanning electron microscopy and quantitative image analysis were performed on the fracture surfaces of the pilot stick on 22 January 2003. Further mechanical testing and microstructural analysis were performed during the following 2 weeks. This report documents the reported findings by ARL.

---

## **2. Objective**

---

The objective of this failure analysis was to determine if any metallurgical evidence existed that suggested that the fractured pilot stick might have contributed to the cause of the crash or whether it occurred as a result of the mishap.

---

## **3. Visual Examination**

---

The pilot cyclic stick was broken into two separate pieces at the weld, attaching the tubular portion to the elbow (figure 1). In figure 1, the fracture surfaces had been covered with foam and taped for protection. Figures 2 and 3 show enlargements of the fractured weld. The fracture occurred along the entire circumference of the weld in the center of the weld bead. It was quite evident that the weld did not have complete penetration in most areas, as evidenced by the relatively smooth surface finish on the elbow and the fact that the elbow did not fracture.



Figure 1. The fractured AH-64D pilot cyclic stick as received by ARL.



Figure 2. Enlargement of the fracture area on the pilot stick.

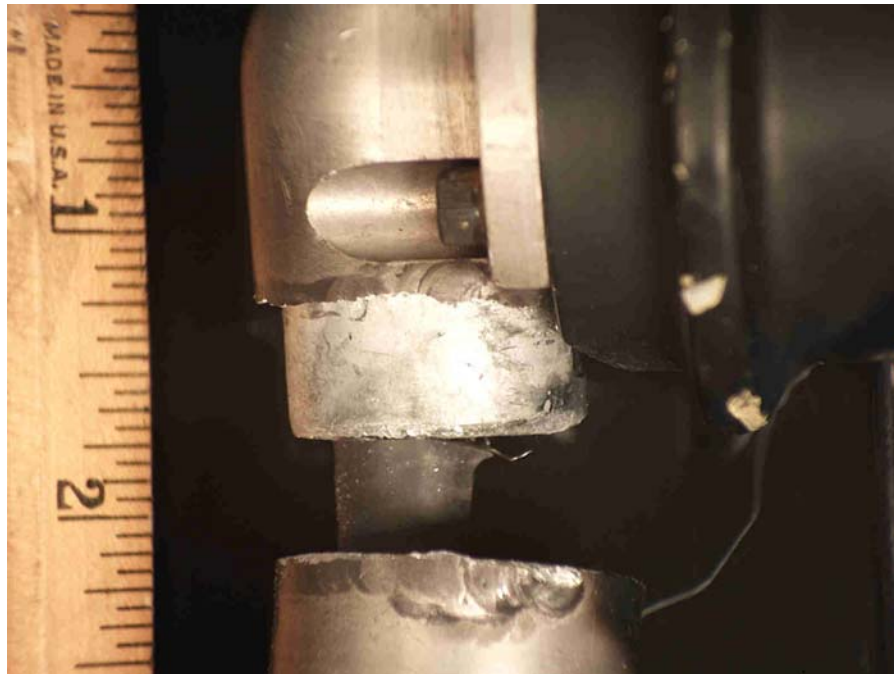


Figure 3. Detail of the pilot stick fractured area.

The copilot cyclic stick was cracked in the same area but did not break into two pieces (figure 4). The bolts that mount the grip to the stick were removed prior to the photograph being taken. Arrows indicate the area of concern in figure 4. Both sticks sustained mishap damage. The copilot stick contained considerably more damage, such that areas of the aluminum tube as well the section containing the control buttons, were dented, gouged, and/or bent, indicative of severe impact loading. However, the copilot cyclic stick, although cracked, was still intact and would most likely require a mechanical testing machine to properly separate the two fracture halves for subsequent examination (figure 5). The important point was that the fractured copilot stick could not easily be broken the rest of the way. Subsequently, the wiring assembly, which ran through the tubular section, was removed, separating the “tube” fracture half from that of the “elbow” fracture half.

Figure 6 shows the tube fracture and the elbow fracture halves, respectively. The lack of penetration appeared as areas without fracture topography, where the as-formed/machined surfaces of the tube and the elbow were clearly discernible. Significant portions of the joint interface also sustained damage and appeared as bright patches without reconcilable topography. Figures 7–9 are enlargements of the weld fracture, showing the lack of penetration and large gas voids. The tube wall thickness was  $\sim 0.095$  in and was used along with the surface morphology characteristics of the fracture to determine weld penetration.

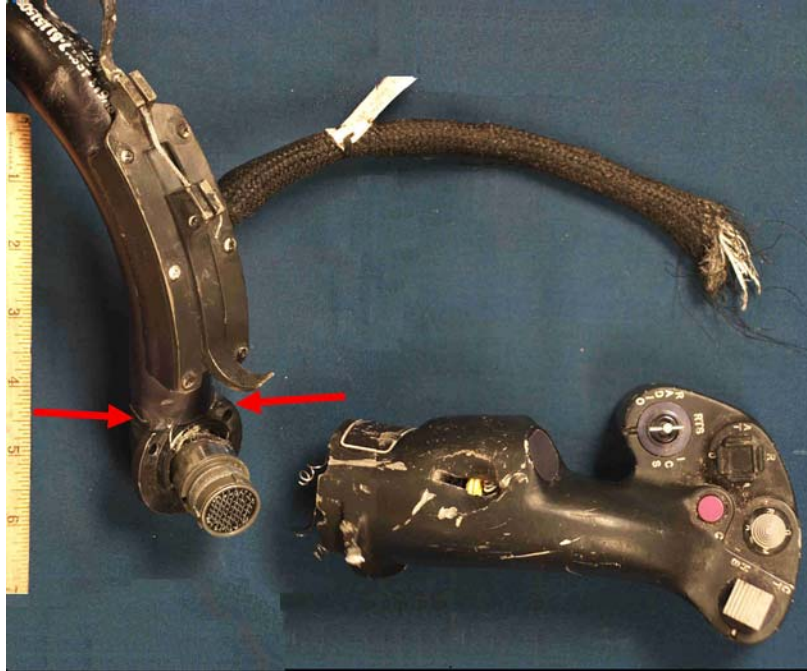


Figure 4. The fractured AH-64D copilot cyclic stick as received by ARL.



Figure 5. Detail of the copilot stick crack at the elbow to tube weld.

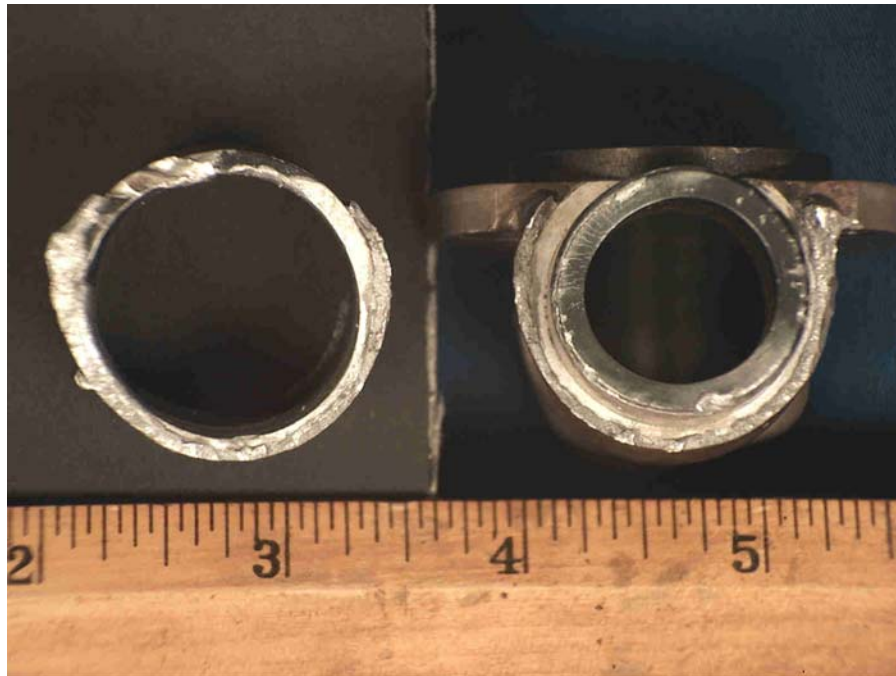


Figure 6. The fracture halves of the pilot cyclic stick.

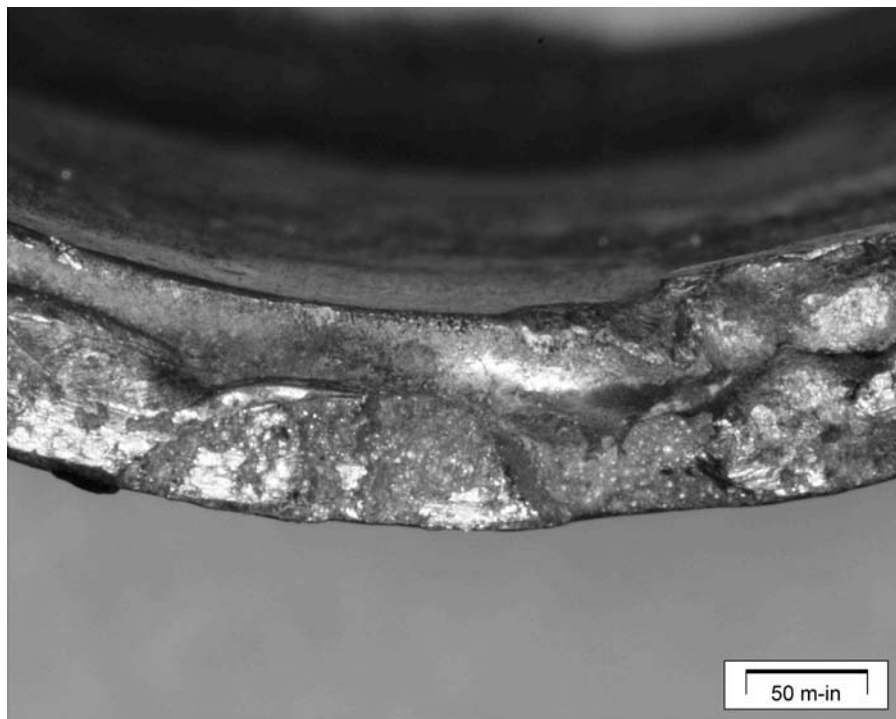


Figure 7. Lack of penetration observed on the tube side fracture half.



Figure 8. Lack of penetration on the tube side at location G on the drawing.

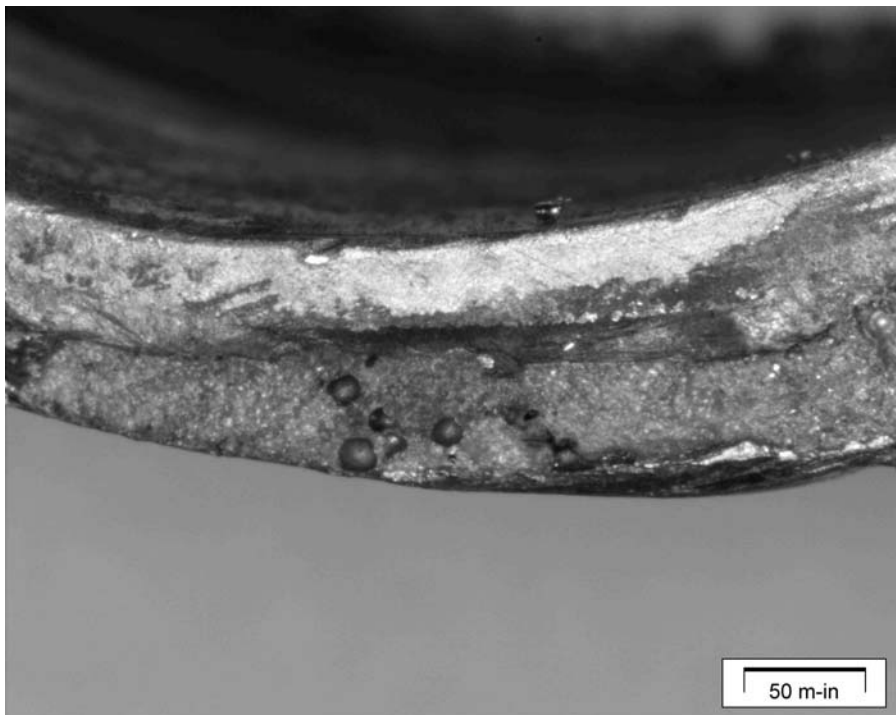


Figure 9. Lack of penetration on the tube side at location F on the drawing.

Figure 10 is a montage of the entire tube weld fracture from which penetration calculations were determined. The cross-sectional area of the welded region was ~40%, as determined by quantitative image analysis. This value was obtained by taking the ratio of the calculated areas between the welded fracture surface and what should have been welded according to the manufacturer's engineering drawing. The area coincides with the tube thickness mating with the elbow below the top of the flange. Figure 11 shows the portion of the tube that should have been welded, while figure 12 depicts the areas left unwelded. The calculated percentage of welded material can be used with the tube thickness to estimate the loading required to fracture the assembly.

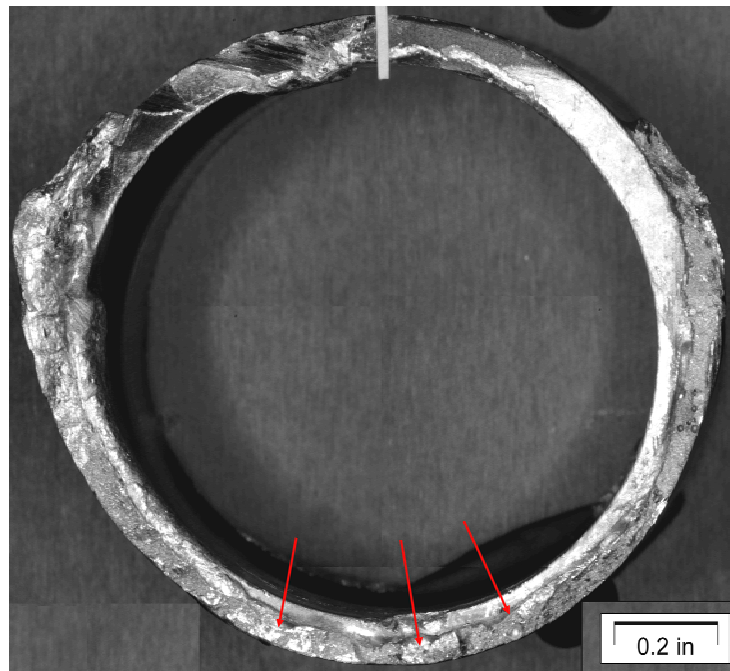


Figure 10. Montage of the fracture surface of the pilot cyclic stick.

Examination of the fracture surfaces did not reveal any evidence of fatigue, such as beach marks, crack arrest marks, or the presence of an “older” appearing fracture surface. An older crack initiation site is usually distinguishable from the remaining fracture in that an oxide layer from atmospheric corrosion typically discolors the area. This was not observed and suggests that the entire fracture occurred all at once.

The failure originated at the root of the weld where there existed incomplete penetration coupled with localized flaws. Arrows in figures 10–12 depict these areas. Figures 13–16 show all three areas in greater detail on the elbow fracture half.

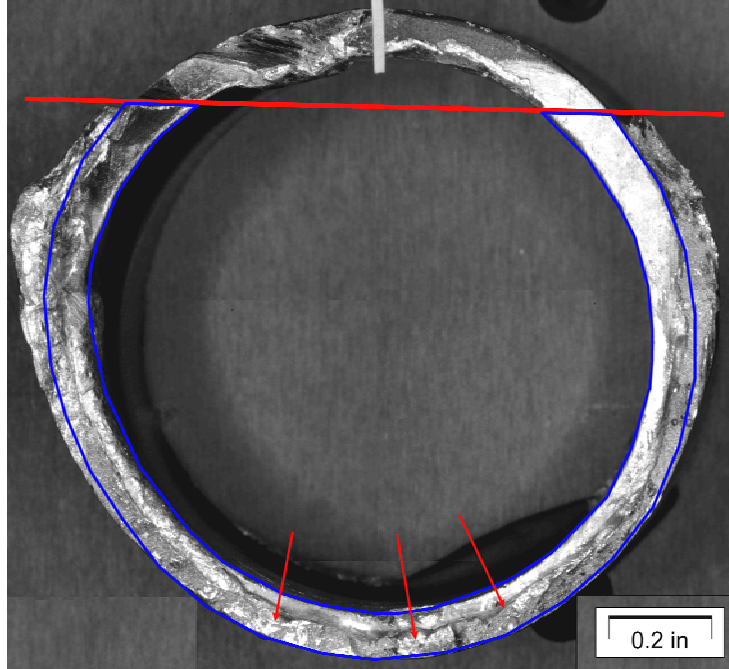


Figure 11. Montage from figure 10 depicting the area that should be welded.

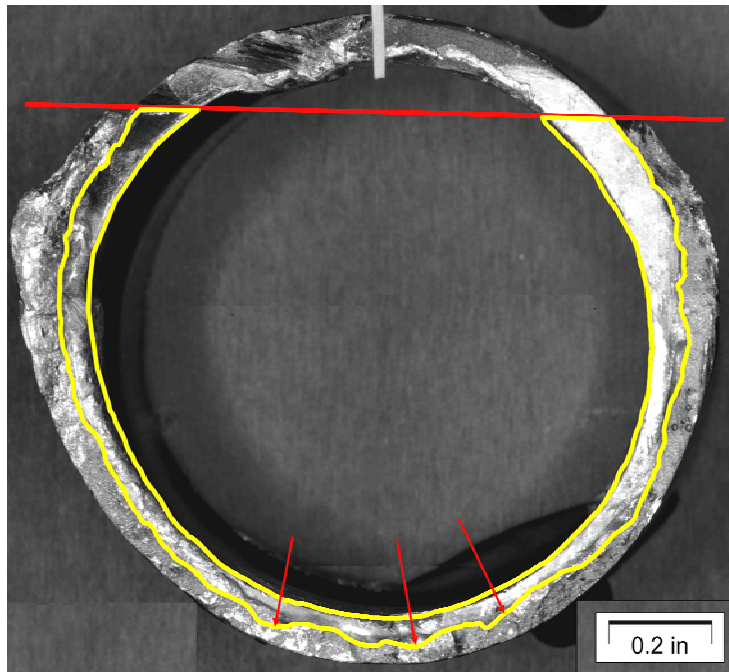


Figure 12. Montage from figure 10 depicting the area that was not welded.



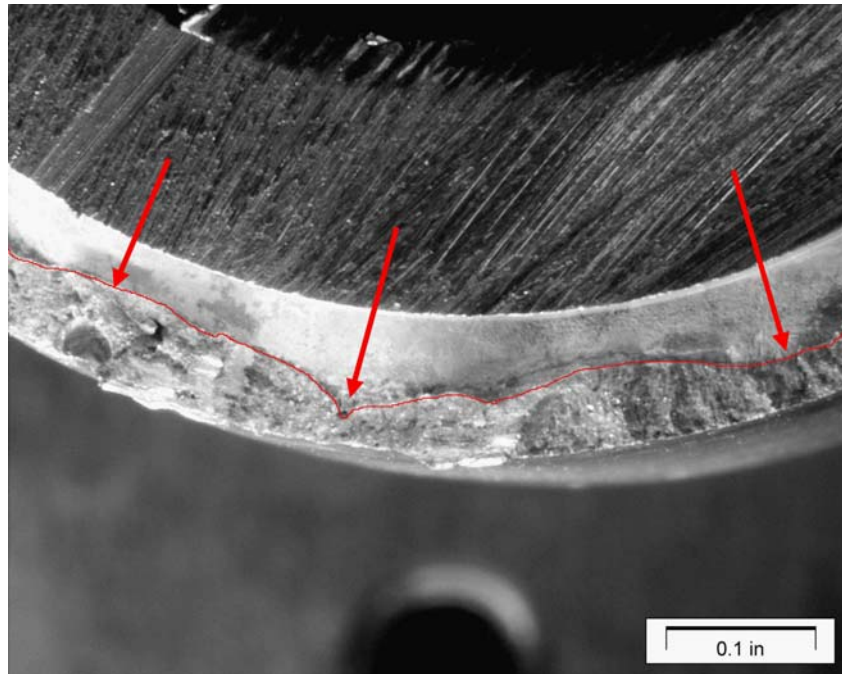


Figure 13. Elbow side fracture half depicting failure origins.

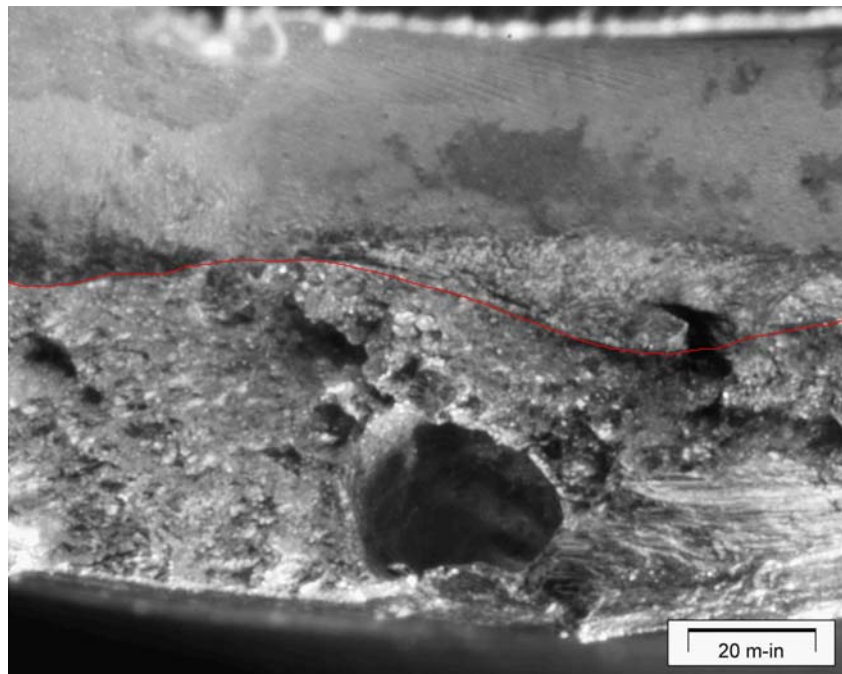


Figure 14. Elbow side fracture half depicting large gas void failure origin, from left side of figure 13.

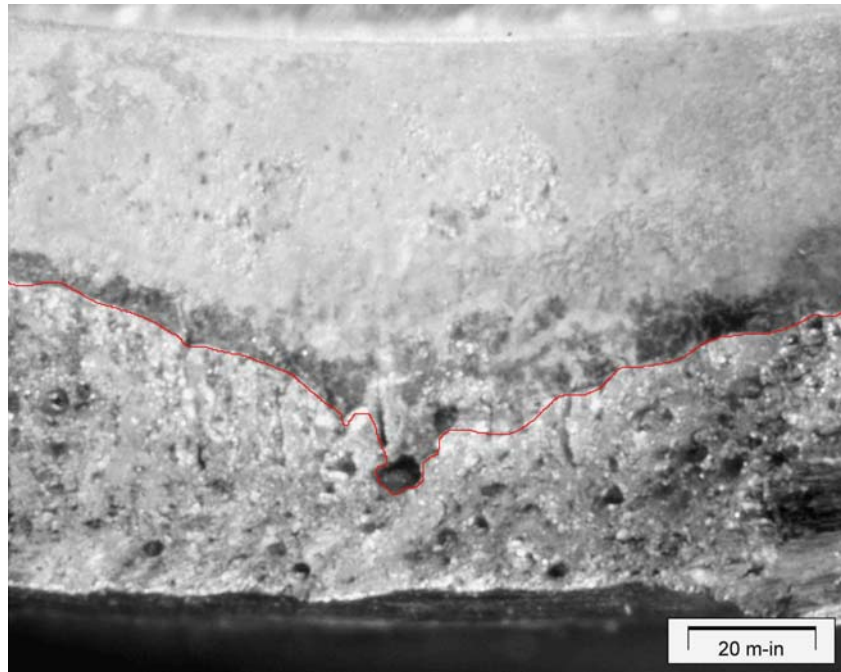


Figure 15. Elbow side fracture half depicting failure origin from cracks and a gas void at the root of the weld, from middle of figure 13.

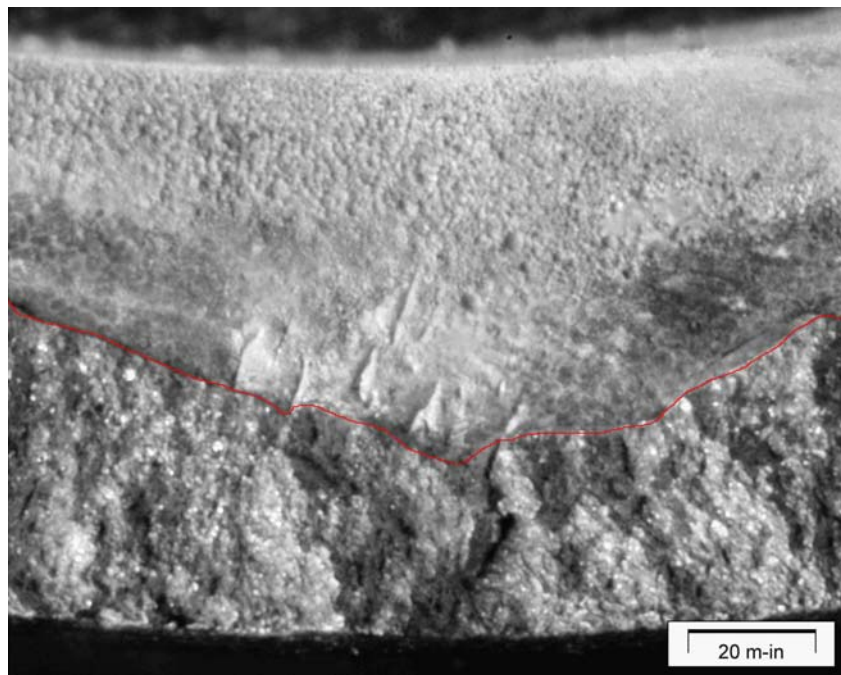


Figure 16. Elbow side fracture half depicting failure origin from large cracks at weld root, from right of figure 13.

---

## 4. Metallographic Examination

---

A cross section of material was taken through the fractured weld on the “tube side” of the fracture as well as on the “elbow side” of the fracture. Both samples were mounted and metallographically prepared for examination. Keller’s reagent was used for etching. Figure 17 is an optical micrograph of the elbow fracture showing the lack of penetration of the weld. To illustrate a weld with 100% penetration, an outline of such a weld (drawn in white) was added to figure 17. The weld bead contained an interdendritic network of aluminum-silicon eutectic (black) and dark etching, Al-Mg<sub>2</sub>Si eutectic between the grains in the heat-affected zone. Figure 18 is an optical micrograph of a cross-section of the tube side of the fractured weld, which did not contain any of the elbow material, also indicating a lack of penetration. Porosity was observed within the weld. Figure 19 represents a micrograph of the tube base material showing a matrix of aluminum solid solution containing particles of Mg<sub>2</sub>Si (black).

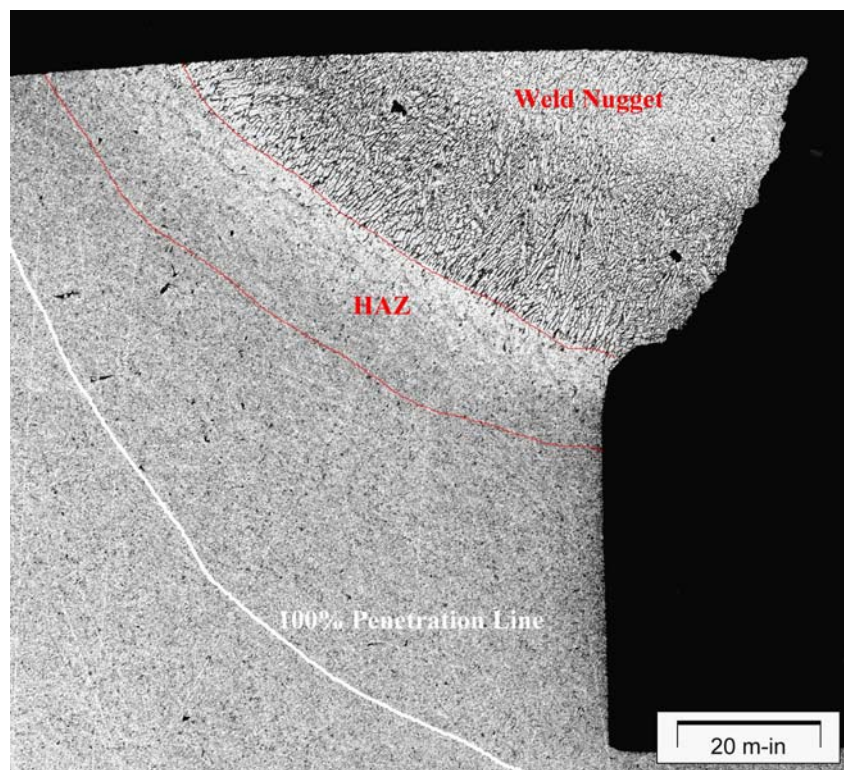


Figure 17. Elbow side cross section through the weld; the white line depicts what would be a 100% penetration weld.

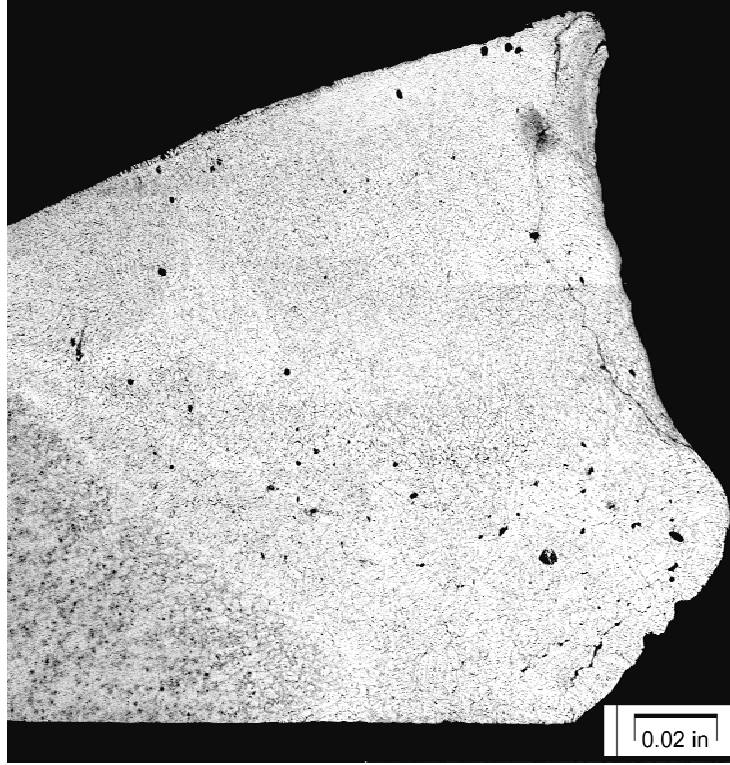


Figure 18. Tube side cross section through the weld.

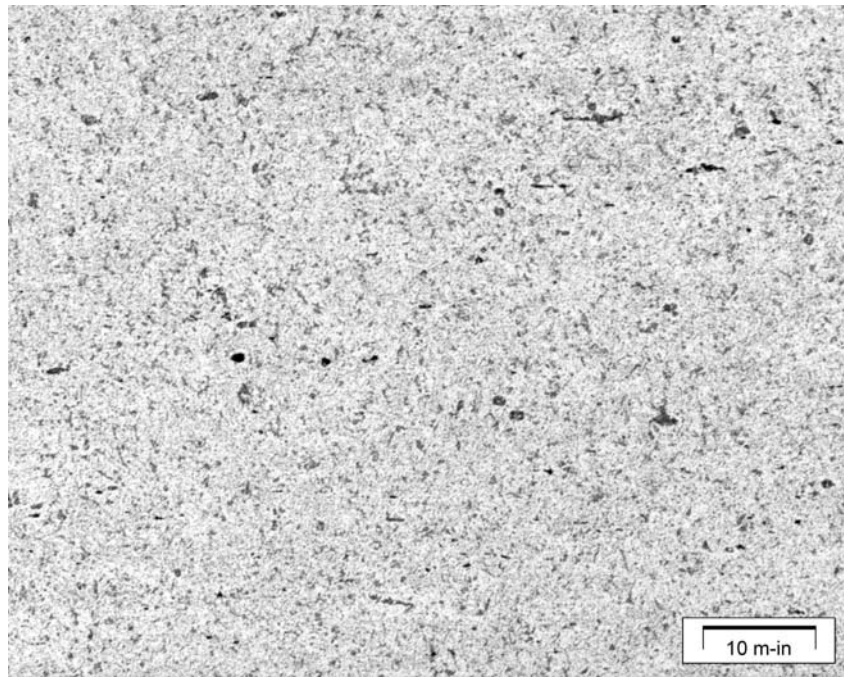


Figure 19. Tube side cross section of base material.

#### 4.1 Eddy Current Electrical Conductivity

The electrical conductivity of the material used to fabricate the tube was used as a means of verifying the heat treatment. The requirement was 6061-T6 and testing was performed in accordance to MIL-H-6088G<sup>1</sup> “Heat Treatment of Aluminum Alloys,” section 4.4.5, “Eddy Current Electrical Conductivity.” The typical conductivity values of 6061-T6 are expressed by percentage of conductivity of the International Annealed Copper Standard (IACS). Measurements were taken on the tube section of the pilot stick and the elbow. The average values are listed in table 1 and compare favorably to the specified requirements.

Table 1. Electrical conductivity for 6061-T6 and the pilot stick tube material.

Alloy	MIL-H-6088G Typical Conductivity (IACS)	Pilot Stick Tube	Pilot Stick Elbow
6061-T6	40.0–47.0	42	45

#### 4.2 Hardness Testing

The hardness of the base material (6061-T6 aluminum) used to fabricate the tube was measured and used as another means to confirm the heat treatment. The hardness of the elbow was also measured. The hardness requirement was 85 HR<sub>E</sub> using the Rockwell hardness E scale, as specified in MIL-H-6088G<sup>1</sup> “Heat Treatment of Aluminum Alloys,” section 4.4.6, “Hardness.” These data are presented in table 2. Hardness testing was performed on metallographic mounts, in accordance with ASTM E 18,<sup>2</sup> incorporating a 100-kg load and a 1/8-in-diameter ball indenter for the E scale and 1000-gm load for the Knoop method. Hardness profiles were also performed with the Knoop Indentation Method across the weldments on both the tube and elbow side. These data are presented in table 3. The shaded values are those visibly within the weld nugget and heat affected zone (HAZ).

#### 4.3 Chemistry

The chemical composition of a sample of the tube and elbow material used to fabricate the cyclic stick was determined using the direct current (DC) plasma emission technique (with Beckman SSVI equipment). The results were compared to QQ-A-200<sup>3</sup> “Aluminum Alloy 6061, Bar, Rod, Shapes, Tube, and Wire, Extruded.” The anodized layer was removed by sanding prior to analysis. The material conformed to the specified chemical composition for 6061 aluminum, as shown in table 4.

<sup>1</sup>MIL-H-6088G. *Heat Treatment of Aluminum Alloys* 1991.

<sup>2</sup>ASTM E 18. Standard Test Method for Rockwell Hardness and Rockwell Superficial Hardness of Metallic Materials. *Annu. Book ASTM Stand.* 1998.

<sup>3</sup>QQ-A-200. Aluminum Alloy 6061, Bar, Rod, Shapes, Tube, and Wire, Extruded. *Aerospace Material Specification, SAE International* 1998.

Table 2. Hardness for 6061-T6 and the pilot stick tube/elbow material.

Alloy	MIL-H-6088G Typical Minimum Hardness (HR <sub>E</sub> )	Pilot Stick Tube (HR <sub>E</sub> )	Pilot Stick Tube (HK)	Pilot Stick Elbow (HR <sub>E</sub> )	Pilot Stick Elbow (HK)
6061-T6	85	85.8	104.6	54.6	70.2
—	85 HR <sub>E</sub> ~ 104 HK	88.8	105.3	58.0	68.9
—	—	87.3	106.7	51.0	65.0
—	—	84.6	105.9	Avg. = 54.5	67.5
—	—	86.6	106.9	—	66.4
—	—	Avg. = 86.6	107.1	—	59.5
—	—	—	108.3	—	63.7
—	—	—	105.7	—	61.6
—	—	—	106.4	—	61.8
—	—	—	106.2	—	63.3
—	—	—	Avg. = 106.3	—	Avg. = 64.8

Table 3. Hardness for 6061-T6 and the pilot stick weldment profiles.

Alloy	MIL-H-6088G Typical Minimum Hardness (HR <sub>E</sub> )	Pilot Stick Tube Weldment Profile (HK)	Pilot Stick Elbow Weldment Profile (HK)
6061-T6	85	108.4	82.8
—	85 HR <sub>E</sub> ~ 104 HK	107.9	80.3
—	—	108.5	75.2
—	—	96.9	76.4
—	—	88.5	71.1
—	—	83.3	68.3
—	—	106.9	66.6
—	—	104.6	61.3
—	—	107.4	58.5
—	—	108.6	57.9

Table 4. Chemical composition of pilot stick tube and elbow material in weight-percent.

Element	QQ-A-200		Tube Material	Elbow Material
	Minimum	Maximum		
Magnesium	0.8	1.2	1.08	1.05
Silicon	0.40	0.8	0.63	0.69
Copper	0.15	0.40	0.29	0.28
Iron	—	0.7	0.19	0.29
Chromium	0.04	0.35	0.058	0.12
Zinc	—	0.25	0.003	0.011
Titanium	—	0.15	0.021	0.028
Manganese	—	0.15	0.0045	0.047
Aluminum	Remainder		Remainder	

The chemical composition of the weld bead was initially determined by quantitative energy dispersing spectroscopy (EDS), within the scanning electron microscope. This method was chosen to obtain relative chemical composition quickly in lieu of wet chemistry techniques to verify the weld rod material. It was not meant to provide absolute values of chemical composition. The differences in the silicon and copper content between the two welding rods were the distinguishing elements used as a basis for comparison. The small concentrations of manganese, magnesium, and zinc did not yield an appreciable peak and therefore did not factor into the overall weight-percentage calculation. Samples of the two possible weld rod materials, AMS 4190 (ER4043) and AMS 4189 (ER4643), were obtained and analyzed to calibrate the EDS system. The spectra obtained are shown in figures 20 and 21. A section of the weld bead on the elbow fitting was polished with 15- $\mu\text{m}$  diamond paste, to remove surface contamination, in preparation for EDS analysis. The spectrum of the weld bead compared favorably to that of ER4643, as figure 22 reveals. Table 5 lists the corresponding numerical values of these EDS analyses.

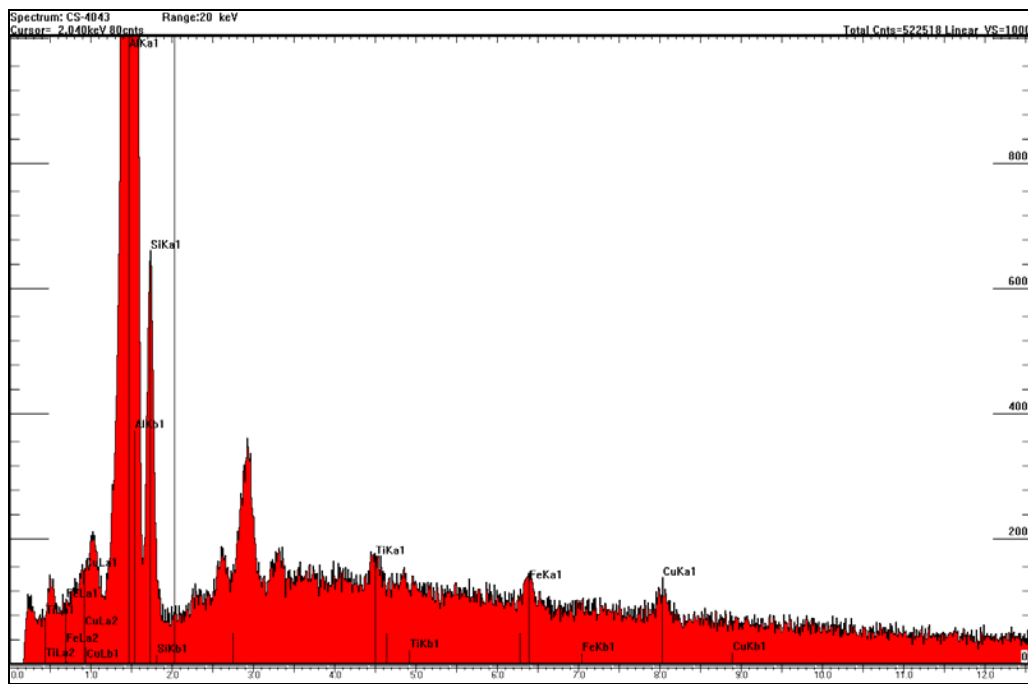


Figure 20. EDS spectrum for the 4043 welding filler rod.

Because it appeared from the hardness data that the pilot stick assembly was not heat-treated, and heat-treatable 4643 weld filler rod was used, a small amount of filler material was painstakingly removed for wet chemical analysis. DC plasma emission spectroscopy (DCP) was used, and the major constituents compared favorably with 4643 filler rod (silicon, copper, and magnesium), confirming the initial analysis. These data are presented in table 6.

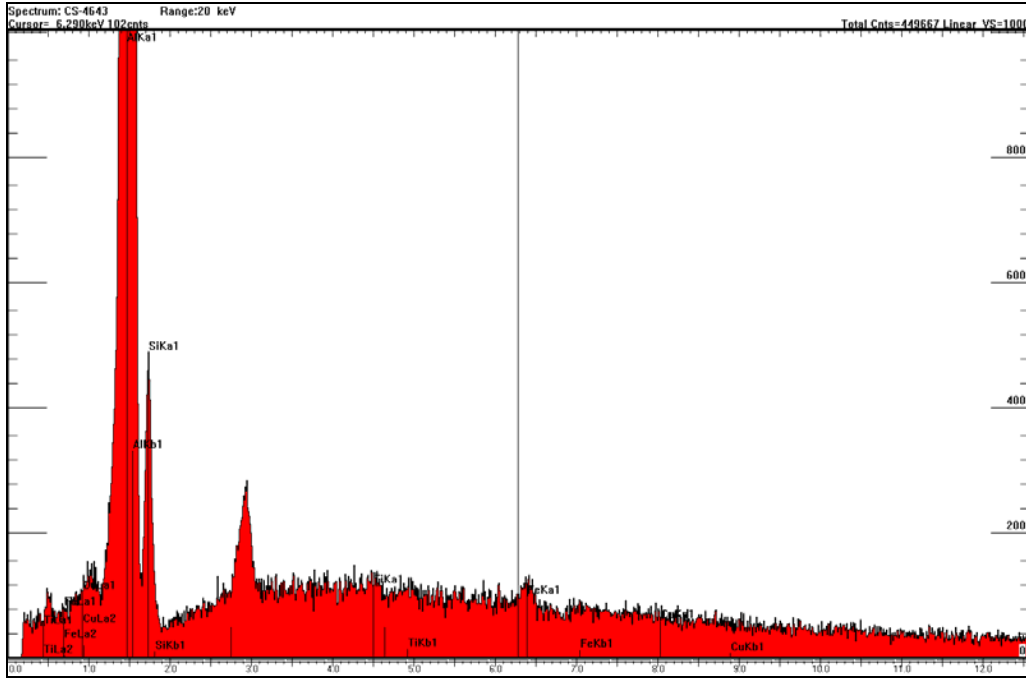


Figure 21. EDS spectrum for the 4643 welding filler rod.

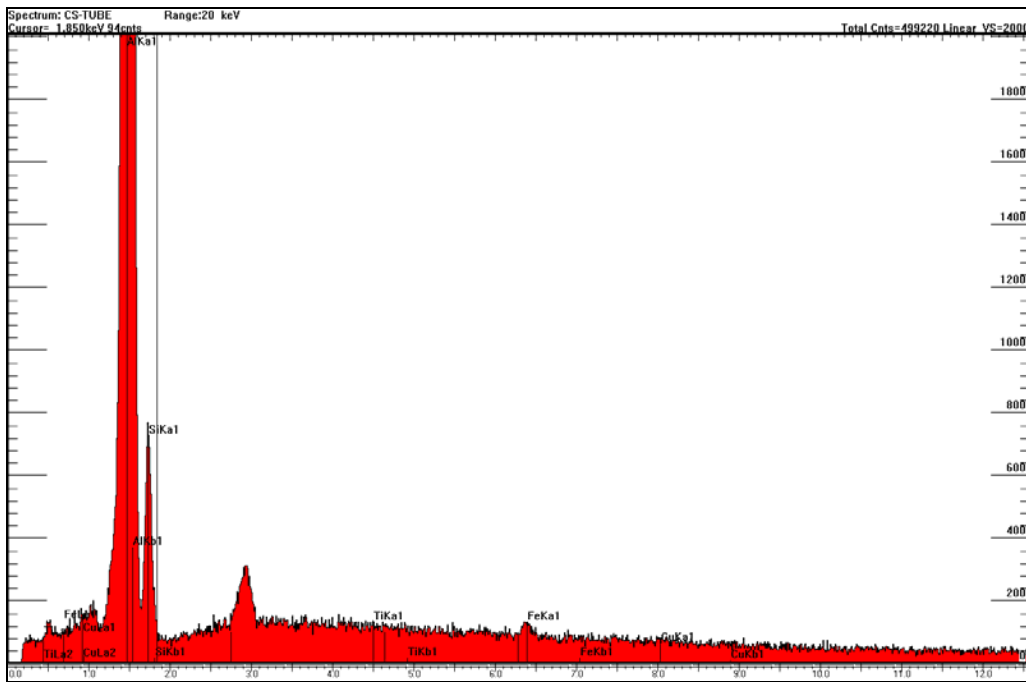


Figure 22. EDS spectrum for the filler metal on the welded pilot stick.



Table 5. Chemical composition of the weld bead and specified weld rods (EDS analysis).

Element	ER4043 AMS 4190	ER4043 Actual Weld Rod (EDS)	ER4643 AMS 4189	ER4643 Actual Weld Rod (EDS)	Actual Weld Bead (EDS)
Aluminum	Balance	Balance	Balance	Balance	Balance
Silicon	4.5–6.0	6.12	3.6–4.6	4.56	4.70
Iron	0.8	0.69	0.8	0.72	0.73
Copper	0.30	0.44	0.10	0.12	0.10
Manganese	0.05	—	0.05	—	—
Magnesium	0.05	—	0.10–0.30	—	—
Chromium	—	—	—	—	—
Zinc	0.10	—	0.10	—	—
Titanium	0.20	0.22	0.15	0.14	0.16

Table 6. Chemical composition of the weld bead and specified weld rods (DCP analysis).

Element	ER4043 AMS 4190	ER4643 AMS 4189	Actual Weld Bead (DCP)
Aluminum	Balance	Balance	Balance
Silicon	4.5–6.0	3.6–4.6	3.63
Iron	0.8	0.8	0.21
Copper	0.30	0.10	0.13
Manganese	0.05	0.05	0.010
Magnesium	0.05	0.10–0.30	0.44
Chromium	—	—	0.031
Zinc	0.10	0.10	0.025
Titanium	0.20	0.15	0.21

---

## 5. Scanning Electron Microscopy (SEM)

---

SEM examination of the fracture surfaces did not reveal any evidence of fatigue, such as beach marks, fatigue striations or a region consistent with an “older” fracture surface. No type of crack arrest marks were found anywhere on the fracture, suggesting that the entire fracture occurred all at once. Additional information substantiating this position was the predominately dimpled fracture morphology, which is indicative of overload conditions (figure 23). At times, these dimples demonstrated directionality, as in figure 24, but only in the late stages of fracture typical of sheared material. There also existed some areas where quasi-cleavage fracture was present (figure 25).

Scanning electron micrographs of the three fracture origins discussed earlier can be observed in figures 26–28 and at higher magnification in figures 29–31. Figure 29 presents the large gas void in greater detail. Due to the inherent gap between the tube and the elbow prior to welding, and the lack of full penetration, there existed areas where the tube material was melted but not

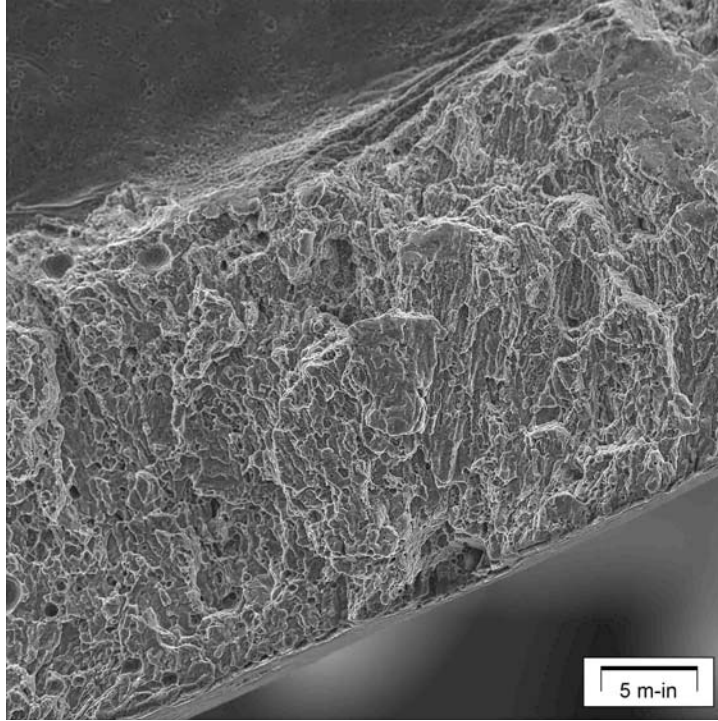


Figure 23. SEM fractograph showing the morphology predominant on the cyclic stick.

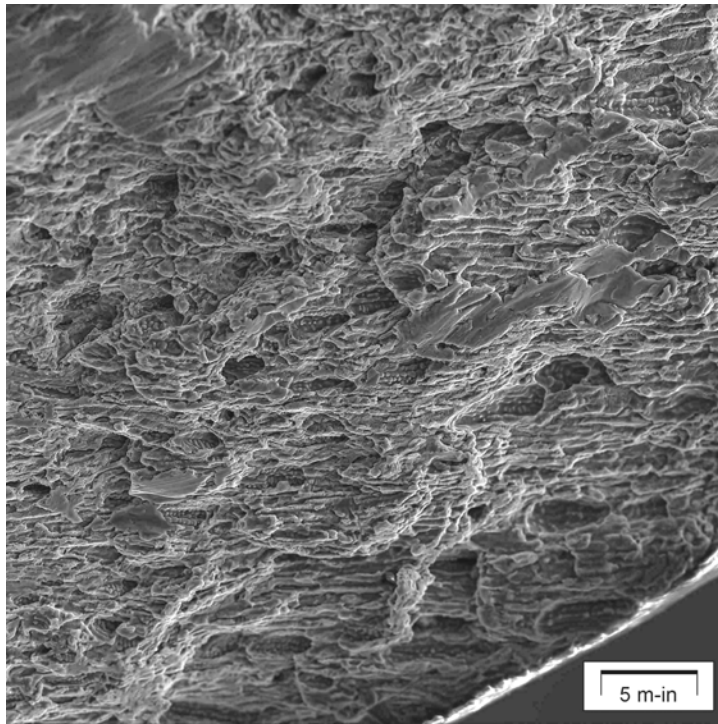


Figure 24. SEM fractograph showing dimpled morphology with directionality.

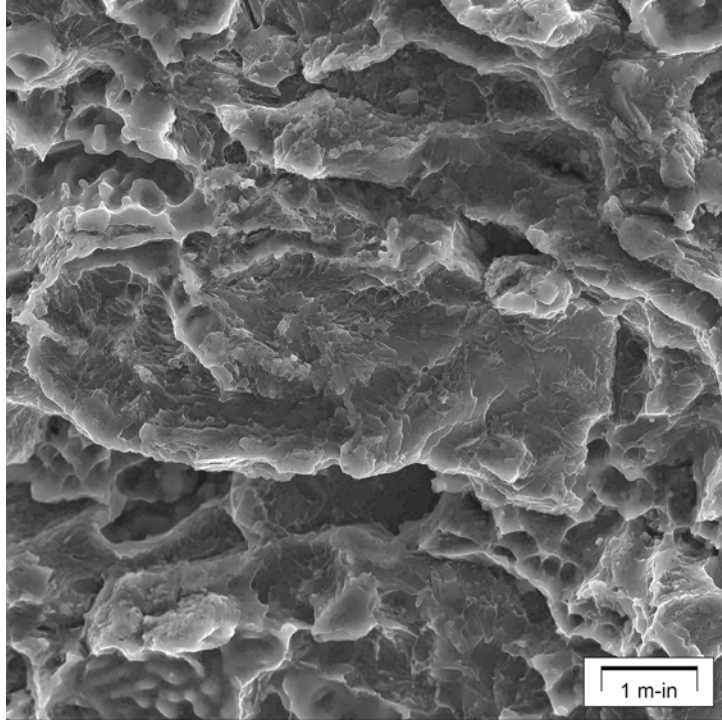


Figure 25. SEM fractograph showing quasi-cleavage morphology.

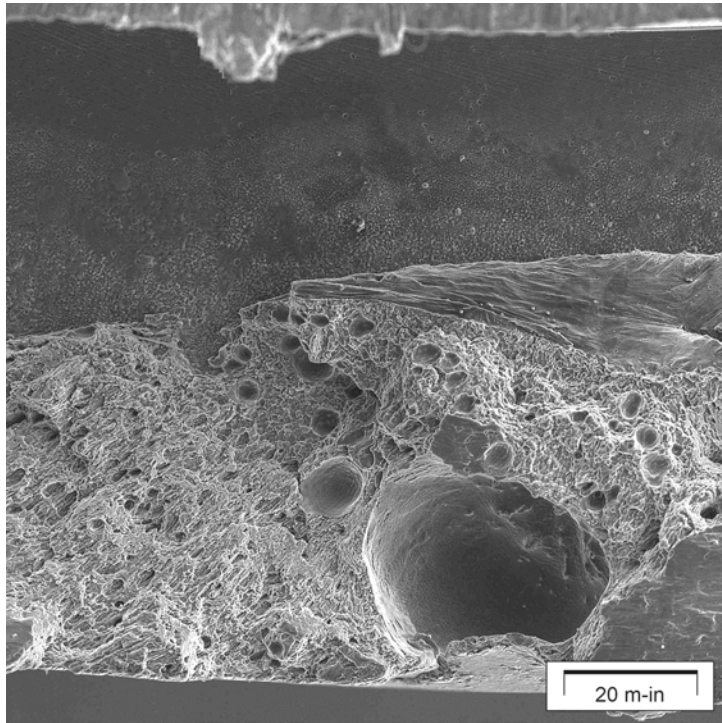


Figure 26. SEM fractograph showing fracture origin from figure 14.

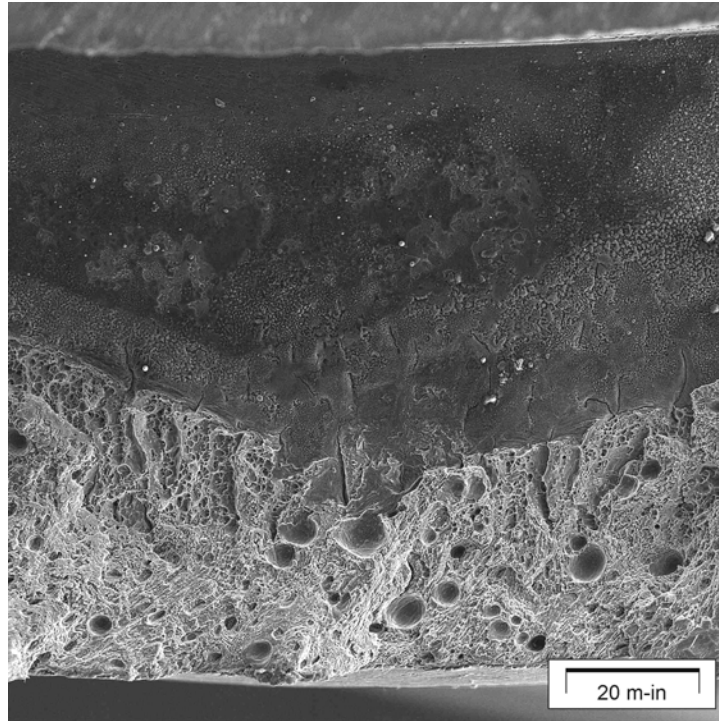


Figure 27. SEM fractograph showing fracture origin from figure 15.

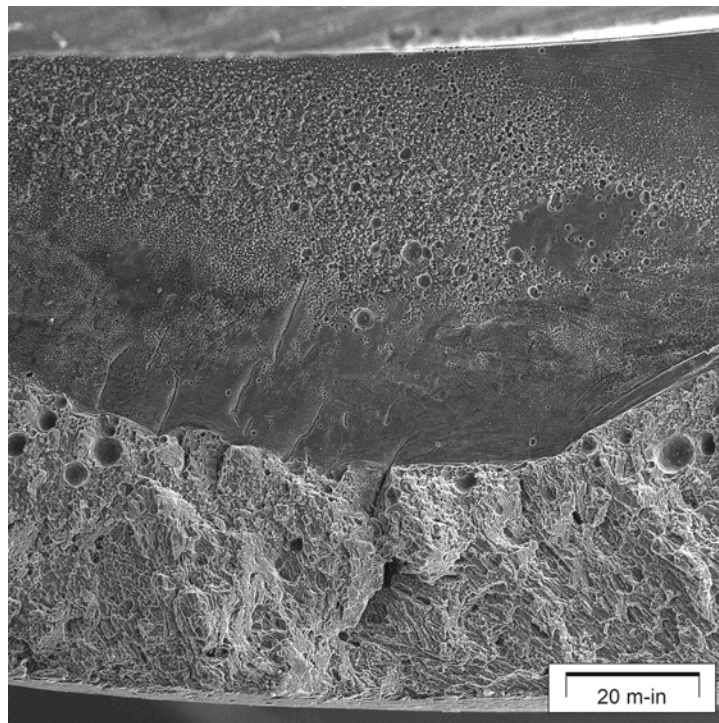


Figure 28. SEM fractograph showing fracture origin from figure 16.

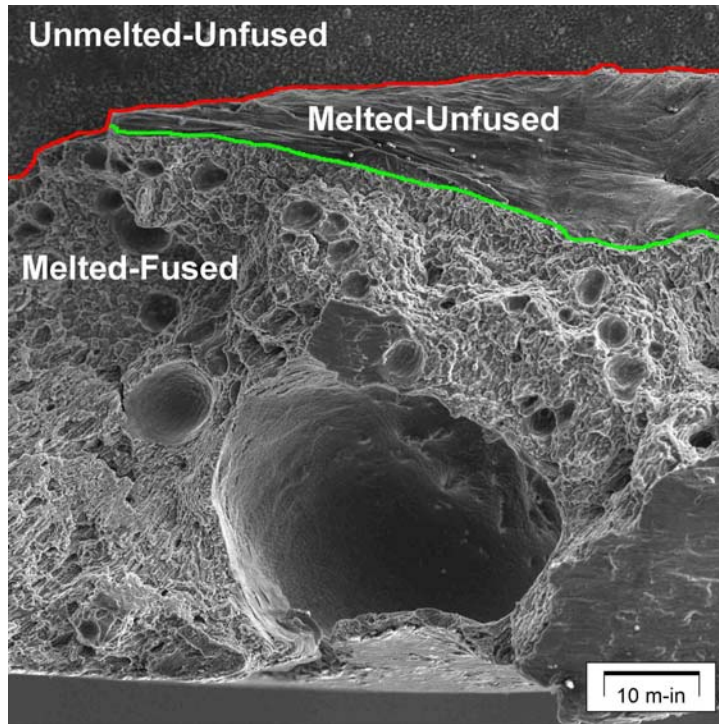


Figure 29. SEM fractograph showing unfused material from figure 26.

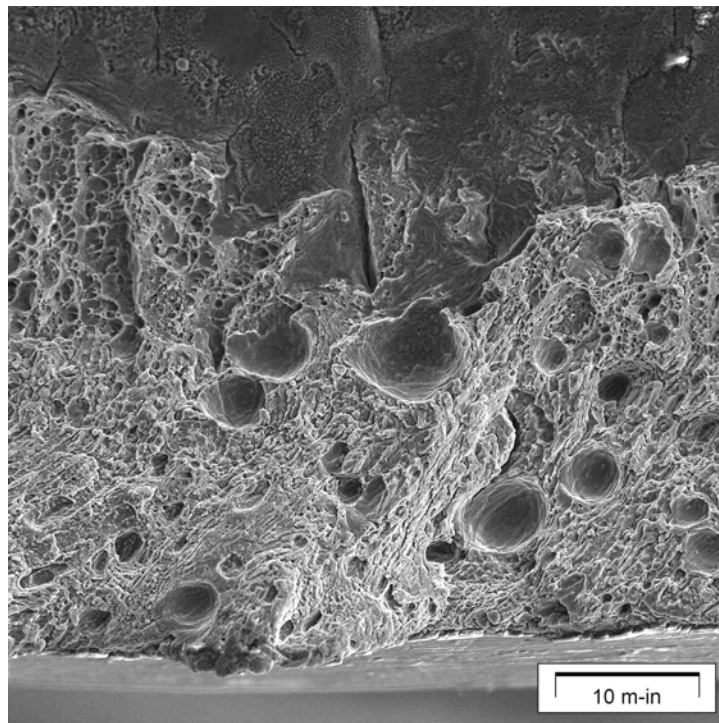


Figure 30. SEM fractograph showing enlargement of figure 27.

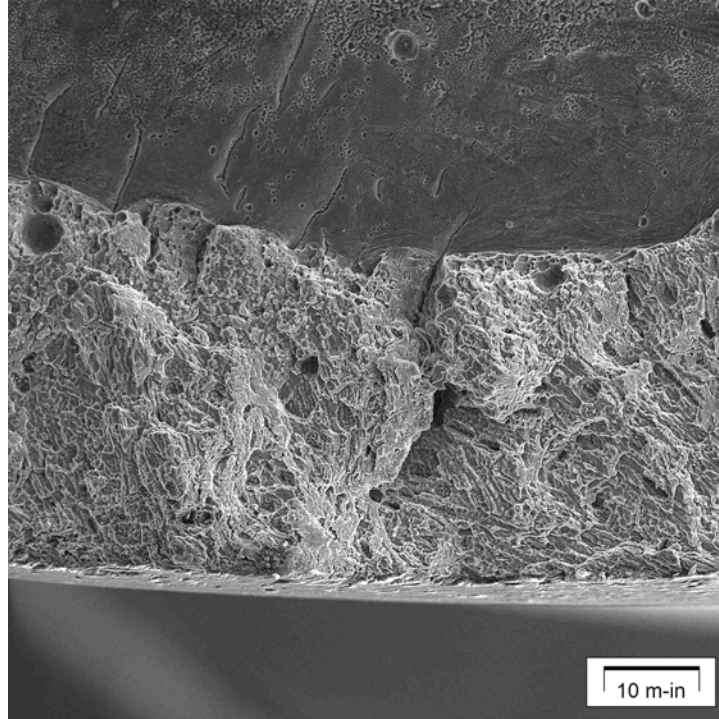


Figure 31. SEM fractograph showing enlargement of figure 28.

fused to the elbow. The melted and fused material left a discernible fracture surface where the parts were separated. This phenomenon can be observed in figure 29. Numerous large gas voids were observed at various locations on the fracture surfaces (figure 32 and 33).

---

## 6. Conclusion

---

The metallurgical findings suggested that the pilot stick fractured during a single event. There was no evidence of fatigue observed on the fracture surface of the pilot stick. The fracture morphology consisted primarily of ductile dimples, indicative of overload conditions. There did exist some areas that were indicative of cleavage fracture but nothing that would suggest a fatigue-induced failure.

---

## 7. Recommendations

---

1. Because the tensile strength of the 4643 weld filler material was only ~20 ksi in the as-welded condition and the area of welded material was ~0.1 in<sup>2</sup>, the loading required to fracture the pilot stick was relatively low. The bending load required to fracture the elbow

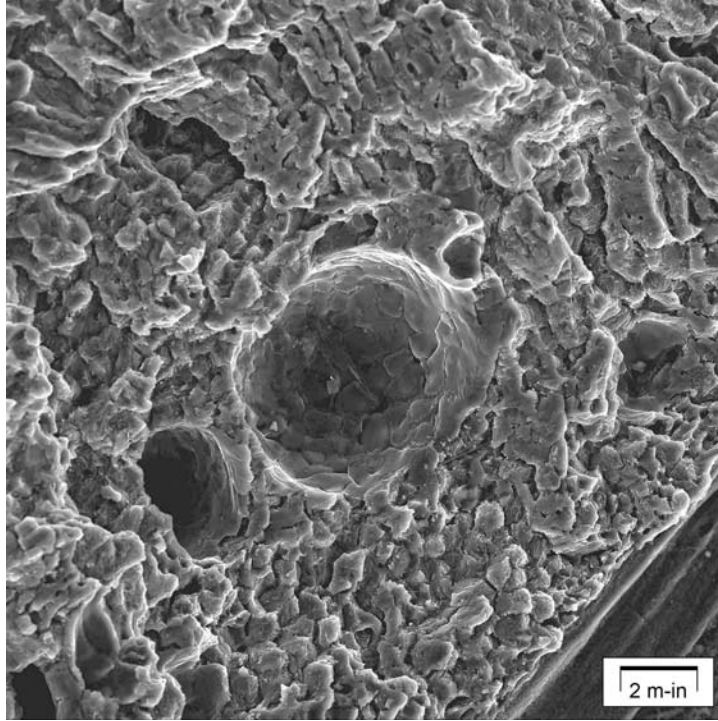


Figure 32. SEM fractograph showing typical gas voids on the surface.

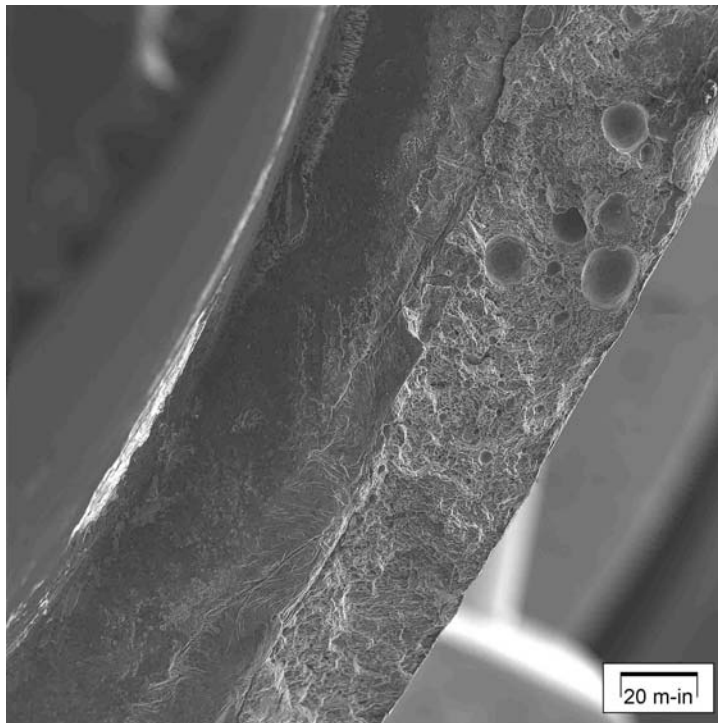


Figure 33. SEM fractograph showing additional typical gas voids on the surface.

from the tube of the pilot stick should be calculated from the data previously mentioned while accounting for the internal flaw (lack of penetration) of the thin walled tube.

2. It is apparent that the pilot cyclic stick should be considered as a critical component and therefore subject to an increased level of inspection to prevent inadequate welds. It is suggested that the weld classification be increased to a class A weld in accordance with the contractor specification HP11-1 requiring 100% radiographic inspection to detect lack of penetration.
3. The copilot stick fracture could be separated in the laboratory without damage to the fractures, by fabricating a special fixture to be inserted in a mechanical testing machine. The crack could then be pulled apart mechanically and examined. The purpose of this would be to provide additional fractographic information. The copilot stick fracture had not been rubbed and/or damaged, and the surface morphology should be more easily reconcilable than the pilot stick.



NO. OF  
COPIES ORGANIZATION

1 DEFENSE TECHNICAL  
(PDF INFORMATION CTR  
ONLY) DTIC OCA  
8725 JOHN J KINGMAN RD  
STE 0944  
FT BELVOIR VA 22060-6218

1 COMMANDING GENERAL  
US ARMY MATERIEL CMD  
AMCRDA TF  
5001 EISENHOWER AVE  
ALEXANDRIA VA 22333-0001

1 INST FOR ADVNCD TCHNLGY  
THE UNIV OF TEXAS  
AT AUSTIN  
3925 W BRAKER LN STE 400  
AUSTIN TX 78759-5316

1 US MILITARY ACADEMY  
MATH SCI CTR EXCELLENCE  
MADN MATH  
THAYER HALL  
WEST POINT NY 10996-1786

1 DIRECTOR  
US ARMY RESEARCH LAB  
AMSRD ARL CS IS R  
2800 POWDER MILL RD  
ADELPHI MD 20783-1197

3 DIRECTOR  
US ARMY RESEARCH LAB  
AMSRD ARL CI OK TL  
2800 POWDER MILL RD  
ADELPHI MD 20783-1197

3 DIRECTOR  
US ARMY RESEARCH LAB  
AMSRD ARL CS IS T  
2800 POWDER MILL RD  
ADELPHI MD 20783-1197

NO. OF  
COPIES ORGANIZATION

ABERDEEN PROVING GROUND

1 DIR USARL  
AMSRD ARL CI OK TP (BLDG 4600)

NO. OF  
COPIES ORGANIZATION

ABERDEEN PROVING GROUND

11 DIR US ARL  
AMSRD ARL WM MC  
BLDG 4600  
V CHAMPAGNE  
S GREND AHL (10 CPS)